


RESEARCH PAPER



Circular RNA circ-LDLRAD3 serves as an oncogene to promote non-small cell lung cancer progression by upregulating SLC1A5 through sponging miR-137

Min Xue^{a*}, Weijun Hong^{a*}, Jun Jiang^b, Fang Zhao^c, and Xiwen Gao ^a

^aDepartment of Respiratory Medicine, Minhang Hospital, Fudan University, Shanghai, China; ^bState Key Laboratory of Genetic Engineering, Shanghai Engineering Research Center of Industrial Microorganisms, School of Life Science, Fudan University, Shanghai, China; ^cDepartment of Laboratory, Minhang Hospital, Fudan University, Shanghai, China

ABSTRACT

Circular RNAs (circRNAs) are closely associated with the development of non-small cell lung cancer (NSCLC); however, it is still unclear whether circular RNA circ-LDLRAD3 participated in the regulation of NSCLC progression. In this study, we found that circ-LDLRAD3 was high-expressed and miR-137 was low-expressed in NSCLC tissues and cells compared to their normal counterparts, which showed negative correlations in NSCLC tissues. Further experiments validated that miR-137 could be sponged and inhibited by circ-LDLRAD3 in NSCLC cells. In addition, knock-down of circ-LDLRAD3 and miR-137 over-expression promoted NSCLC cell apoptosis, and inhibited cell proliferation and invasion. Similarly, upregulation of circ-LDLRAD3 or miR-137 ablation had opposite effects on the above cell functions. Besides, the glutamine transporter SLC1A5 was validated to be the downstream target of circ-LDLRAD3 and miR-137, and upregulated circ-LDLRAD3 increased SLC1A5 expression levels by downregulating miR-137. Furthermore, the effects of downregulated circ-LDLRAD3 on cell proliferation, apoptosis and mobility were all reversed by knocking down miR-137 and overexpressing SLC1A5. Taken together, this *in vitro* study found that knock-down of circ-LDLRAD3 inhibited the development of NSCLC by regulating miR-137/SLC1A5 axis.

ARTICLE HISTORY

Received 8 February 2020
Revised 18 June 2020
Accepted 25 June 2020

KEYWORDS

Non-small cell lung cancer; circular RNA circ-LDLRAD3; miR-137; SLC1a5

Introduction

Non-small cell lung cancer (NSCLC) is a common malignancy among human beings [1,2], and accounts for about 80–85% of all lung cancer cases [3]. As the results of its complicated pathogenesis and unclear molecular mechanisms, current therapies for NSCLC have been largely limited [4–6]. The solution for this problem is to delineate the potential mechanisms of NSCLC progression. Recent studies identified the post-transcriptional regulators, circular RNAs (circRNAs), were closely associated with the development of NSCLC [7–9]. For example, circ-PRMT5 served as an oncogene in regulating NSCLC progression [10] and circ-PTPRA suppressed NSCLC metastasis by sponging miR-96-5p [11]. Specifically, circular RNA circ-LDLRAD3 (hsa_circ_0006988) is an intragenic gene located at chr11: 36248634–36248980, which had recently been identified as an oncogene in pancreatic cancer [12,13]. Of note, circ-LDLRAD3 served as a diagnostic biomarker for pancreatic cancer [12] and knock-down of circ-LDLRAD3 suppressed the development of pancreatic cancer progression [13]. However, it is still unclear whether circ-LDLRAD3 involves in the regulation of NSCLC pathogenesis.


Another type of post-transcriptional regulators, microRNAs (miRNAs), is also pivotal for the regulation of NSCLC progression [14–16]. Previous studies found that

miR-608 promoted NSCLC cell apoptosis by targeting TFAP4 [16], and upregulation of miR-330 promoted epithelial-mesenchymal transition (EMT) of NSCLC cells [17]. MiR-137 has been reported to act as a tumour suppressor in the development of multiple cancers, including pancreatic cancer [13], colorectal cancer [18] and NSCLC [19]. Notably, miR-137 slowed down cell proliferation in human NSCLC cells by targeting SRC3 [19] and inhibited NSCLC cell migration via downregulating bone morphogenetic protein-7 (BMP7) [20]. In addition, circRNAs participated in the regulation of cell functions by modulating miRNAs in a competing endogenous RNA (ceRNA) dependent manner [21–23], and researchers found that miR-137 could be sponged by circ-LDLRAD3 in pancreatic cancer cells [13].

The glutamine transporter solute carrier family A1 member 5 (SLC1A5) is crucial for the transportation and metabolism of L-glutamine (Gln) [24], which has long been known to be essential for cancer cell growth [25,26], and researchers validated that SLC1A5 promoted the development of cancers by promoting Gln metabolism [27–29]. Of note, SLC1A5 participated in the regulation of NSCLC progression [30] and inactivation of SLC1A5 inhibited NSCLC cell viability by decreasing Gln consumption [31,32]. Besides, upregulation of SLC1A5 promoted cell migration and invasion in papillary thyroid cancer [29]. In addition, SLC1A5 could be inhibited by various miRNAs [33–

CONTACT Xiwen Gao  gaowixwen@sina.com  Department of Respiratory Medicine, Minhang Hospital, Fudan University, Shanghai 201199, China; Fang Zhao  zhao_fang552@163.com  Department of Laboratory, Minhang Hospital, Fudan University, 170 Xin-Song Road, Shanghai 201199, China

*Means co-first authors

 Supplemental data for this article can be accessed [here](#).

35]. Specifically, SLC1A5 was proved to be the downstream target of miR-137 and involved in the regulation of ferroptotic cell death in melanoma [35]. The above literatures enlightened us that circ-LDLRAD3 might regulate SLC1A5 levels in NSCLC cells in a miR-137 dependent manner; however, the detailed mechanisms are still unknown.

Based on the above information, this study was designed to investigate the role of circ-LDLRAD3/miR-137/SLC1A5 axis in the modulation of NSCLC development. This work will broaden our knowledge of NSCLC pathogenesis, and give more insights into the underlying mechanisms of NSCLC progression.

Materials and methods

Clinical specimens

The NSCLC tissues (N = 60) and their paired adjacent normal tissues (N = 60) were collected from the NSCLC patients underwent surgical resection of primary tumour at Minhang Hospital, Fudan University from 2013 to 2017. The above clinical specimens were frozen at -70°C refrigerator for further experiments. The clinicopathological features (age, gender, TNM stage, pathological type, smoking status and lymphatic metastasis) are listed in Table 1. The informed consent forms were obtained from all the participants and all the procedures for clinical experiments in this study were approved by the ethics committee of the Minhang Hospital, Fudan University.

Cell culture and vectors transfection

The NSCLC cell lines (A549, H1299 and Calu-3) and human bronchial epithelial cell line (HBE) were obtained from American Type Culture Collection (ATCC, USA). The above cells were cultured in the Roswell Park Memorial Institute 1640 Medium (HyClone, UT) and incubated under the standard culture conditions (5% CO_2 , 37°C). The cells were cultured for vectors transfection until the cell confluency reached about 70–80%. The miR-NC, miR-137 mimic (5'-TTA TTG CTT AAG AATACGCGT AG-3') and inhibitor (5'-CTA CGC GTA TTC TTA AGC AAT AA-3') were designed and synthesized by Sangon Biotech (Shanghai, China) according to the experimental procedures provided by the previous studies [36,37]. The small interfering RNA (siRNA) for circ-LDLRAD3 was designed

by Sangon Biotech (Shanghai, China) to knock down circ-LDLRAD3, and the siRNA sequences for vector construction were listed as follows: sense (5'-GGA TCA AGA TTG AAG CAT-3') and antisense (5'-UUA CAU GCG AUU ACG UAC AAU UGA-3'). The full sequences for SLC1A5 and circ-LDLRAD3 were introduced into pcDNA-3.1 vectors to generate overexpressed SLC1A5 (OE-SLC1A5) and circ-LDLRAD3 (OE-circ-LDLRAD3) vectors by GenePharma (Shanghai, China). The miR-NC (5 nM), miR-137 mimic (5 nM), miR-137 inhibitor (5 nM), circ-LDLRAD3 siRNA (10 nM), OE-circ-LDLRAD3 (10 nM) and OE-SLC1A5 (7 nM) were delivered into A549 and H1299 cells by using the LipofectamineTM 2000 transfection reagent following the manufacturer's instruction. At 48 h post-transfection, the cells were prepared for further analysis.

Real-time qPCR

The total RNA for clinical tissue specimens and cell lines were extracted by using the TRIzol reagent (Invitrogen, USA) in keeping with the manufacturer's instructions. For circ-LDLRAD3 quantification, the circular RNA was enriched and pretreated with RNase R enzyme (3 U/ μg) for 20 min at 37°C to eliminate linear LDLRAD3. The total RNA was reversely transcribed into complementary DNA (cDNA) by using the TaqMan Reverse Transcription Reagents (Applied Biosystems, USA). The commercial One Step TB GreenTM PrimeScriptTM RT-PCR kit (Takara, Japan) was used to determine the expression levels of the involved genes in this study. All the primer sequences for Real-Time qPCR are listed in Table 2.

Western blot analysis

The total proteins were extracted from the cells and clinical tissues by using the radio-immunoprecipitation assay (RIPA) lysis buffer (Beyotime, Shanghai, China) in keeping with the manufacturer's protocol. The bicinchoninic acid (BCA) protein assay was conducted to measure the protein concentrations. After that, the proteins (40 μg per well) were separated by 10% sodium dodecyl sulphate-polyacrylamide gel electrophoresis (SDS-PAGE) and transferred onto polyvinylidene fluoride (PVDF) membranes. The PVDF membranes were blocked with 5% skimmed milk and probed with primary antibodies against β -actin (1:2000, #ab8227, Abcam, UK), Cyclin D1 (1:1000, #ab40754, Abcam, UK), CDK2 (1:2000, #ab32147, Abcam, UK), p27 (1:1500, #ab215434, Abcam, UK), cleaved Caspase-3 (1:1000, #ab32042, Abcam, UK), Bax (1:1000,

Table 1. The clinical characteristics of the NSCLC patients in this study.

Parameters	Group	Total
Age	≤ 65	34
	> 65	26
Gender	Male	20
	Female	40
TNM Stage	I	12
	II	18
	III	16
	IV	14
Pathological Type	Squamous	15
	Adenocarcinoma	20
	Large Cell Lung Cancer	25
Smoking status	Non-smoker	24
	Smoker	16
	Heavy smoker	20
Lymphatic Metastasis	No	34
	Yes	26

Table 2. The primer sequences for Real-Time qPCR.

Gene	Primer sequences (strand)
β -actin	Forward: 5'-CTCCATCCTGGCCTCGTGT-3'
	Reverse: 5'-GCTGCTACCTTCACCGTTC-3'
U6	Forward: 5'-GACTATCATATGCTTACCGT-3'
	Reverse: 5'-GGGCAGGAAGAGGGCCTAT-3'
Circ-LDLRAD3	Forward: 5'-CTTGCTGGACAGAGAAC-3'
	Reverse: 5'-CATGAGGTTGTTCCGCTTC-3'
LDLRAD3 mRNA	Forward: 5'-CAGCCATTCCTGCTGTC-3'
	Reverse: 5'-TCATGCACCACAGTCACAT-3'
SLC1A5	Forward: 5'-CAACCTGGTGCAGCAGCCTT-3'
	Reverse: 5'-GCACCCTCATGTTGACGGTG-3'
miR-137	Forward: 5'-AGGTCAGGCAGCATCGGAA-3'
	Reverse: 5'-AGGCCCTGTGGATATCGTCCAG-3'

#ab53154, Abcam, UK), Bcl-2 (1:1500, #ab196495, Abcam, UK), N-cadherin (1:1000, #ab19348, Abcam, UK), Vimentin (1:1500, #ab137321, Abcam, UK) and SLC1A5 (1:2000, #ab187708, Abcam, UK), respectively. Thereafter, the membranes were incubated with the horseradish peroxidase-conjugated secondary antibody (1:3000, Abcam, UK) for 2 h at room temperature. The ECL luminescence reagent (ThermoFisher Scientific, USA) was used to visualize the protein bands.

Flow cytometry (FCM)

After transfection of the above vectors into NSCLC cells (A549 and H1299), the cells were cultured for 48 h and cell apoptosis ratio was determined by using the Annexin V/Propidium iodide (PI) double staining kit (HaiGene Corporation, China) following the manufacturer's instructions. The cells were harvested and incubated with the Annexin V-FITC and PI double staining solution for 15–20 min at room temperature without light. After that, the flow cytometer (FCM) machine (BD Biosciences, NJ, USA) was employed to measure cell apoptosis ratio.

Cell counting kit-8 (CCK-8) assay

The cell proliferation abilities in NSCLC cells (A549 and H1299) were determined by using the commercial CCK-8 kit (YEASEN, Shanghai, China) according to the manufacturer's instructions. Briefly, the NSCLC cells were transfected with the above vectors and seeded onto the 96-well plates at the density of 3000 cells per well. After cell culture for 0 h, 24 h, 48 h, 72 h and 96 h, respectively, the CCK-8 solution was added into the wells and incubated with the cells for 2 h at 37°C. The optical density (OD) values were determined at the wavelength of 450 nm to reflect cell proliferation abilities.

Transwell assay

The transwell assay was used to evaluate cell invasion abilities in NSCLC cells. The transwell plates (Corning Co-Star, USA) were purchased to finish the test. The NSCLC cells were cultured in the upper compartment in serum-free Roswell Park Memorial Institute 1640 (RPMI-1640) Medium at the density of 2×10^4 cells per well. The lower chamber was added with cell culture medium containing 10% foetal bovine serum (FBS) as chemotaxin. After culturing the cells for 12 h, the filters were fixed with 4% paraformaldehyde and stained with 0.1% crystal violet to visualize the cells. The cell numbers were counted and photographed under light microscope.

Dual-luciferase reporter gene system

The binding sites of miR-137, circ-LDLRAD3 and 3'UTR regions of SLC1A5 mRNA were predicted by using the online starBase software (<http://starbase.sysu.edu.cn/>). Specifically, the targeting sites in SLC1A5 mRNA located in chr19:47278161–47278183, and miR-137 bound to circ-LDLRAD3 at chr11:36223457–36223481, which contained 5'-3' junction regions of circ-LDLRAD3. One specific binding sequence for circ-LDLRAD3 and SLC1A5 mRNA was mutated, respectively. The wild-type (Wt) and mutant (Mut) circ-LDLRAD3, and SLC1A5 mRNA were cloned into the

pmirGLO Expression Vector by Sangon Biotech (Shanghai, China). The miR-NC (5 nM) and miR-137 mimic (5 nM) were co-transfected with the above vectors (5 nM) into A549 and H1299 cells by using the Lipofectamine™ 2000 transfection reagent in keeping with the manufacturer's protocol. After 24 h, the relative luciferase activity in the cells was determined by the dual-luciferase reporter gene system (Promega, USA).

Colony formation assay

The colony formation assay was employed to measure colony formation abilities in NSCLC cells. The NSCLC cells were transfected with the involved vectors and seeded into the 24-well plates at the density of 1000 cells per well. After 14 days culture, the cells were fixed with paraformaldehyde and stained with crystal violet (Beyotime Technology, China). The numbers of the colonies containing at least 10 cells were photographed and counted under the light microscope.

Terminal deoxynucleotidyl transferase (TdT)-mediated dUTP nick-end labelling (TUNEL) assay

The commercial TUNEL kit (Thermo Fisher Scientific, USA) was employed to detect apoptotic cells in NSCLC cells transfected with the involved vectors. The cells were stained with the diaminobenzidine (DAB) reaction mixture supplied by the kit. The nuclei DNA was stained with 4',6-diamidino-2-phenylindole (DAPI). The light microscope was employed to observe TUNEL-positive cells to evaluate cell apoptosis. The apoptosis ratio of NSCLC cells were quantified by using the Image J software.

Statistical analysis

The data in this study were collected and represented as Means \pm Standard Deviation (SD). All the data were analysed by using the Statistical Product and Service Solutions (SPSS, version 18.0) software. The comparisons between two groups were conducted by the Student's t-test. The unpaired Analysis of Variance (ANOVA) method was employed to compare the means from multiple groups. The Pearson correlation analysis was conducted to analyse the correlations among circ-LDLRAD3, miR-137 and SLC1A5 mRNA in cancer specimens collected from NSCLC patients. The figures were depicted by using the GraphPad Prism 7.0 software. ' p value < 0.05 ' was regarded as statistical significance.

Results

The expression status of circ-LDLRAD3 and miR-137 in NSCLC tissues and cells

The NSCLC tissue specimens (N = 60) and their paired adjacent normal tissue samples (N = 60) were collected, and Real-Time qPCR was performed to determine the levels of circ-LDLRAD3 and miR-137 in the above clinical samples. The results showed that circ-LDLRAD3 was high-expressed (Fig. 1A), while miR-137 was low-expressed (Fig. 1B) in NSCLC tissues compared to their paired normal tissues. Besides, the Pearson correlation analysis results showed that the levels of circ-LDLRAD3 and miR-137 negatively correlated in NSCLC tissues (Fig. 1C). In

addition, we investigated whether the levels of circ-LDLRAD3 and miR-137 correlated with the clinical parameters, such as age, gender, TNM stage, pathological type, smoking status and lymphatic metastasis. The results showed that circ-LDLRAD3 was

relatively high-expressed and miR-137 was low-expressed in patients with high-grade TNM stage (III and IV) (Fig. 2A,C) and lymphatic metastasis (Fig. 2B,D) comparing to their counterparts. However, the levels of circ-LDLRAD3 and miR-137 had

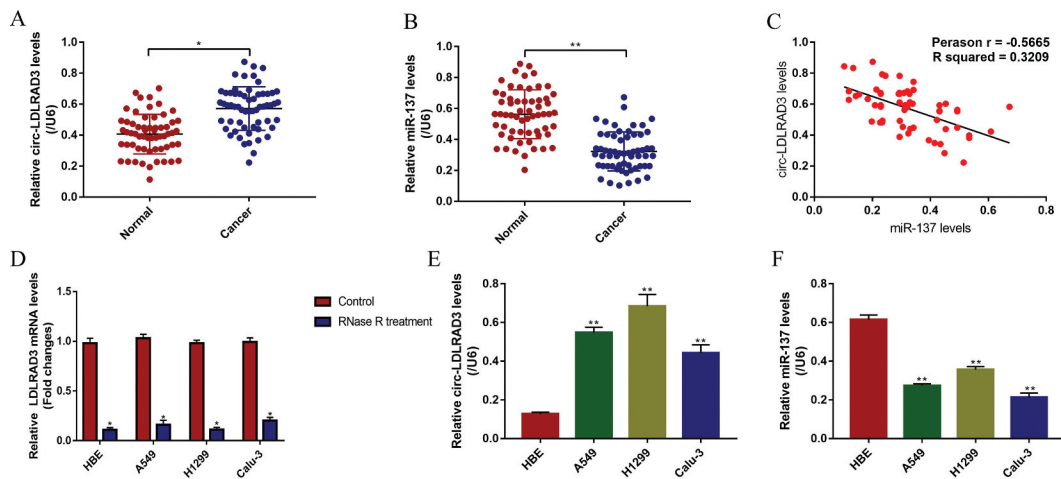


Figure 1. The expression status of circ-LDLRAD3 and miR-137 in clinical specimens and NSCLC cell lines. The cancer tissues and their paired adjacent normal tissues were collected from 60 NSCLC patients. Real-Time qPCR was conducted to determine the levels of (A) circ-LDLRAD3 and (B) miR-137 in clinical tissues collected from NSCLC patients. (C) Pearson correlation analysis was performed to analyse the correlation between circ-LDLRAD3 and miR-137 in NSCLC tissues. Real-Time qPCR was employed to detect the levels of (D) linear LDLRAD3 mRNA (normalized by β -actin), (E) circ-LDLRAD3 and (F) miR-137 in NSCLC cell lines (A549, H1299 and Calu-3) and human bronchial epithelial cell line (HBE), respectively. Each experiment repeated at least 3 times. * $p < 0.05$, ** $p < 0.01$.

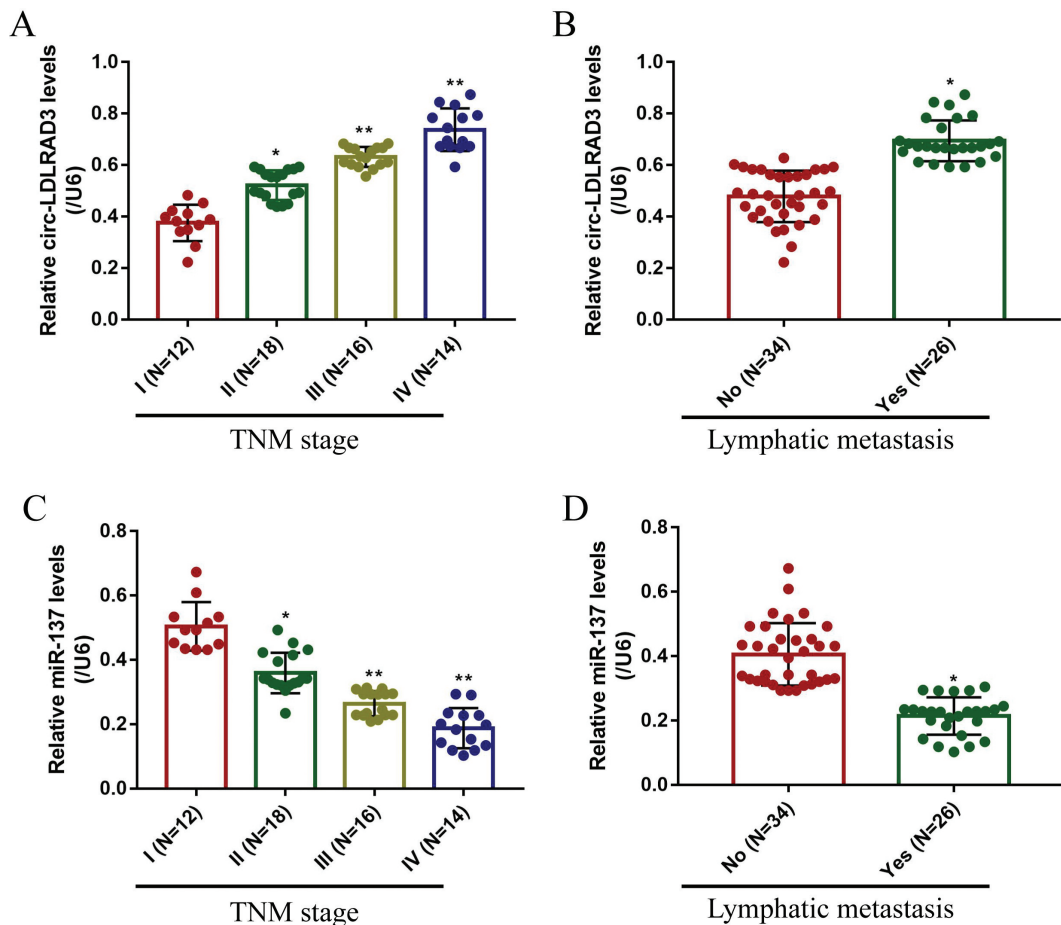


Figure 2. The expression levels of circ-LDLRAD3 and miR-137 in NSCLC tissues collected from patients with different clinicopathological features. Circ-LDLRAD3 was high-expressed in patients with (A) high-grade TNM stage and (B) lymphatic metastasis. MiR-137 levels were determined by Real-Time qPCR in NSCLC patients with different (C) TNM stages and (D) lymphatic metastasis status. Each experiment repeated at least 3 times. * $p < 0.05$, ** $p < 0.01$.

nothing to do with other clinical parameters including age, gender, smoking history and pathological type (Figs. S1 and S2). Furthermore, the *in vitro* experiments were conducted to determine the levels of circ-LDLRAD3 and miR-137 in normal human bronchial epithelial (HBE) cells and NSCLC cells. The results showed that overexpressed circ-LDLRAD3 (Fig. 1E) and downregulated miR-137 (Fig. 1F) were observed in A549 (fold changes: 3.43 and 0.48), H1299 (fold changes: 4.45 and 0.58) and Calu-3 (fold changes: 3.24 and 0.42) compared to the normal HBE cells, and the RNase R enzyme degraded linear LDLRAD3 mRNA in the cells, which partly supported the above clinical results (Fig. 1D). In addition, the expression levels of linear LDLRAD3 mRNA were not affected between normal HBE cells and NSCLC cells (Fig. S6). Of note, since higher expression levels of circ-LDLRAD3 were observed in A549 and H1299 cells, compared to the Calu-3 cells, the A549 and H1299 cells were chosen for further experiments in this study.

The effects of circ-LDLRAD3 on NSCLC cell apoptosis, proliferation and invasion

Since the ectopic circ-LDLRAD3 levels were observed in both NSCLC tissues and cells, we next investigated the role of circ-

LDLRAD3 in the regulation of NSCLC cell functions, including cell apoptosis, proliferation and mobility. To achieve this, the circ-LDLRAD3 downregulation vectors (10 nM, 48 h) and circ-LDLRAD3 overexpressed vectors (10 nM, 48 h) (OE-circ-LDLRAD3) were synthesized and transfected into A549 and H1299 cells (Fig. S3A), respectively. The results showed that we successfully overexpressed (Fold changes: 3.98 and 4.01, vs. Control group) and downregulated (Fold changes: 0.312 and 0.408, vs. Control group) circ-LDLRAD3 in NSCLC cells (Fig. S3A). The flow cytometry (FCM) results showed that knock-down of circ-LDLRAD3 significantly increased the apoptosis ratio in both A549 and H1299 cells, and circ-LDLRAD3 overexpression did not affect NSCLC cell apoptosis (Fig. 3A,B), which suggested that knock-down of circ-LDLRAD3 induced NSCLC cell apoptosis. Similarly, knock-down of circ-LDLRAD3 slowed down NSCLC cell proliferation comparing to the control group, and overexpression of circ-LDLRAD3 promoted cell proliferation in both A549 and H1299 cells (Fig. 3C,D). Furthermore, the effects of circ-LDLRAD3 on NSCLC cell invasion were also determined by transwell assay (Fig. 3E,F). The results showed that NSCLC cell invasion was inhibited by circ-LDLRAD3 ablation, and circ-LDLRAD3 overexpression promoted cell invasion in A549 and H1299 cells (Fig. 3E,F).

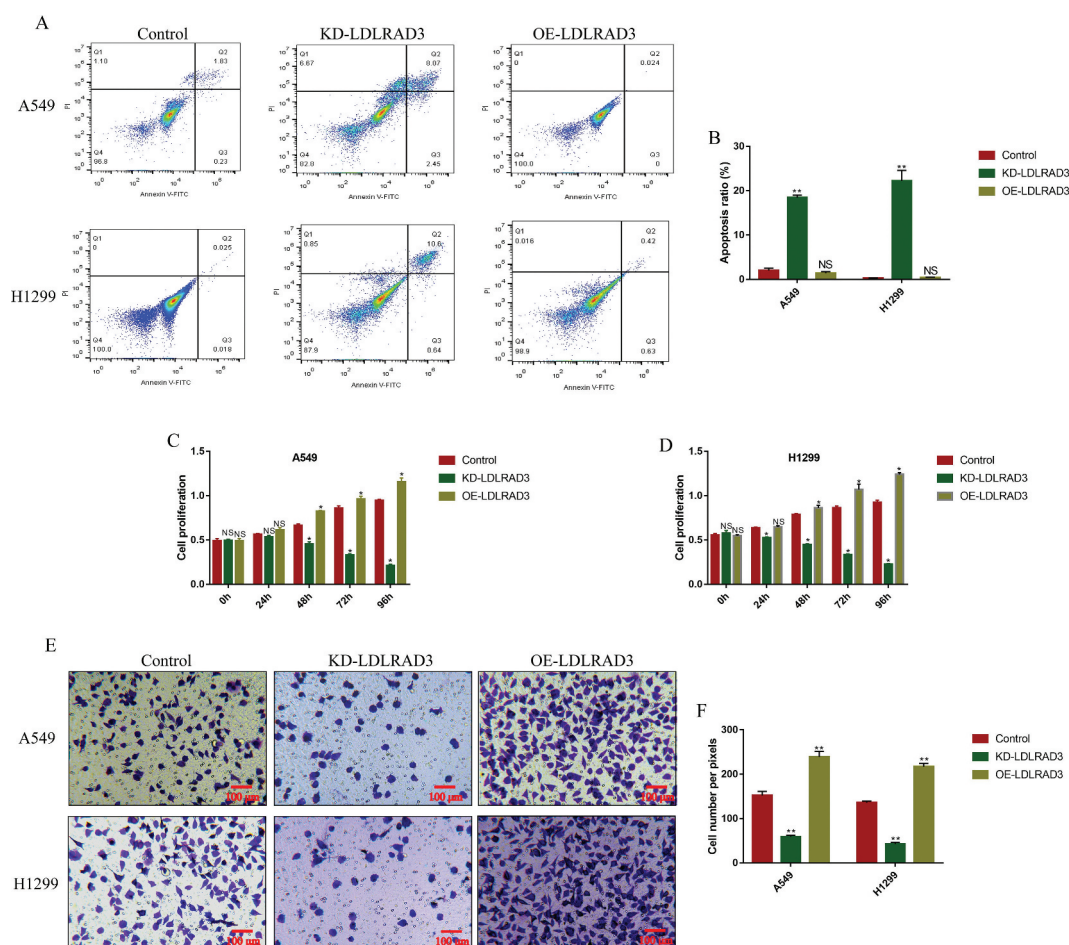


Figure 3. Circ-LDLRAD3 affected cell apoptosis, proliferation and invasion in NSCLC cell lines. The NSCLC cell lines (A549 and H1299) were transfected with circ-LDLRAD3 overexpression and knock-down vectors, respectively. (A, B) FCM was used to examine cell apoptosis ratio in NSCLC cells. (C, D) CCK-8 assay was employed to detect NSCLC cell proliferation. (E, F) Transwell assay was performed to examine cell invasion abilities in NSCLC cells. Each experiment repeated at least 3 times. * $p < 0.05$, ** $p < 0.01$ and 'NS' represented 'No statistical significance'.

MiR-137 regulated NSCLC cell apoptosis, proliferation and epithelial-mesenchymal transition (EMT)

Further experiments were conducted to investigate the effects of miR-137 on NSCLC cell functions, including cell apoptosis, proliferation and EMT. The miR-137 mimic (5 nM, 48 h) and inhibitor (5 nM, 48 h) were successfully transfected into A549 and H1299 cells to overexpress (Fold changes: 3.21 and 3.42, vs. Control group) and knock down (Fold changes: 0.32 and 0.28, vs. Control group) miR-137 (Fig. S3B). The CCK-8 assay results showed that miR-137 overexpression inhibited cell proliferation in A549 and H1299 cells in a time-dependent manner (Fig. 4A,B). Consistently, knock-down of miR-137 promoted NSCLC cell proliferation (Fig. 4A,B). The above results were verified by further Western Blot analysis, which showed that overexpression of miR-137 significantly decreased the expression levels of Cyclin D1 (fold changes: 0.61 and 0.72, vs. Control group) and CDK2 (fold changes: 0.34 and 0.65, vs. Control group), and promoted p27 expressions (fold changes: 2.12 and 3.08, vs. Control group) in both A549 and H1299 cells (Fig. 4C-F). Conversely, knock-down of miR-137 promoted Cyclin D1 (fold changes: 1.23 and 1.48, vs. Control group) and CDK2 (fold changes: 1.37 and 1.29, vs. Control group), and slightly inhibited p27 (fold changes: 0.87 and 0.97, vs. Control group) in A549 and H1299 cells (Fig. 4C-F), which indirectly supported that miR-137 inhibited NSCLC cell proliferation.

In addition, the expression levels of pro-apoptosis proteins (cleaved Caspase-3 and Bax) and anti-apoptosis protein (Bcl-2) were also determined by Western Blot analysis in NSCLC

cells to evaluate cell apoptosis. The results showed that miR-137 overexpression increased the expression levels of cleaved caspase-3 (fold changes: 1.45 and 1.36, vs. Control group) and Bax (fold changes: 1.39 and 1.32, vs. Control group), inhibited Bcl-2 expressions (fold changes: 0.34 and 0.28, vs. Control group) in both A549 and H1299 cells, while miR-137 down-regulation inhibited cleaved caspase-3 (fold changes: 0.61 and 0.58, vs. Control group) and Bax (fold changes: 0.72 and 0.38, vs. Control group), and promoted Bcl-2 (fold changes: 1.23 and 1.31, vs. Control group) expressions in NSCLC cells (Fig. 5A-D). Furthermore, miR-137 regulated epithelial-mesenchymal transition (EMT) of NSCLC cells (Fig. 5E-H). Specifically, the results showed that the expression levels of N-cadherin (fold changes: 0.23 and 0.52, vs. Control group) and Vimentin (fold changes: 0.65 and 0.34, vs. Control group) were decreased by overexpressing miR-137 in A549 and H1299 cells, knock-down of miR-137 promoted N-cadherin (fold changes: 1.67 and 1.59, vs. Control group) and Vimentin (fold changes: 1.54 and 1.38, vs. Control group) expressions in NSCLC cells (Fig. 5E-H), which suggested that miR-137 inhibited EMT in NSCLC cells.

The regulating mechanisms of circ-LDLRAD3, miR-137 and SLC1A5

Previous study reported that miR-137 could be sponged and inhibited by circ-LDLRAD3 [13], which was also validated in this study. The online StarBase software (<http://starbase.sysu.edu.cn/>) predicted the binding sites of miR-137 and

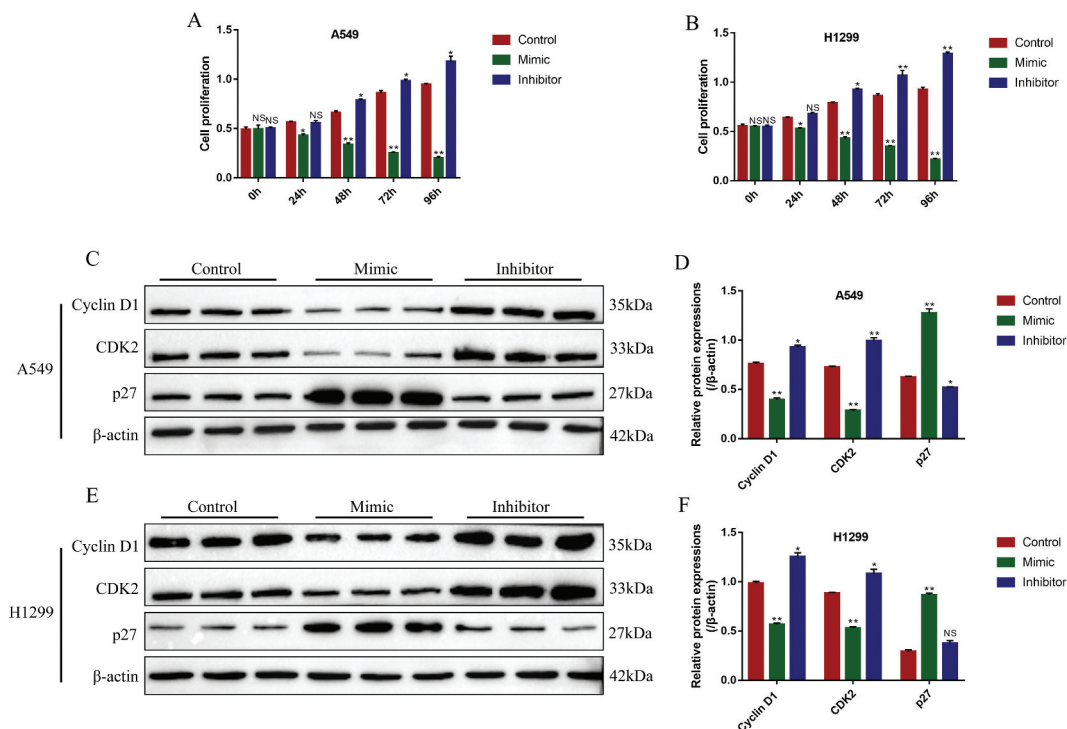


Figure 4. MiR-137 inhibited NSCLC cell proliferation. (A, B) The NSCLC cells (A549 and H1299) were transfected with miR-137 mimic and inhibitor, respectively, cell proliferation was determined by using CCK-8 assay. Western Blot was employed to determine the expression levels of proliferation associated proteins (Cyclin D1, CDK2 and p27) in (C, D) A549 cells and (E, F) H1299 cells, respectively. Each experiment repeated at least 3 times. * $p < 0.05$, ** $p < 0.01$.

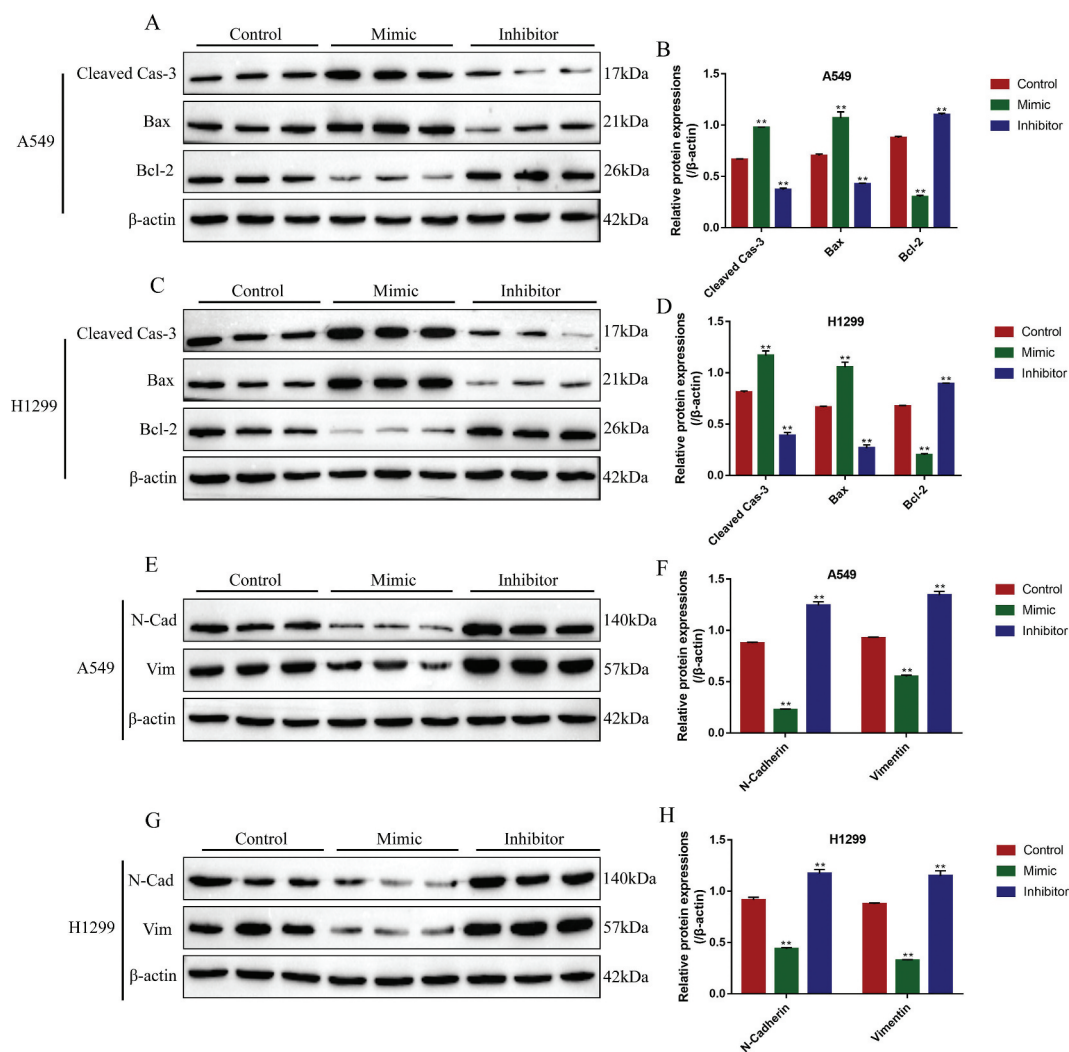


Figure 5. The influences of miR-137 on NSCLC cell apoptosis and epithelial-mesenchymal transition (EMT). The NSCLC cells (A549 and H1299) were transfected with miR-137 mimic and inhibitor, respectively. The apoptosis associated proteins (cleaved Caspase-3, Bax and Bcl-2) were determined by Western Blot in (A, B) A549 cells and (C, D) H1299 cells. The biomarkers for EMT (N-cadherin and Vimentin) were measured in (E, F) A549 cells and (G, H) H1299 cells. Each experiment repeated at least 3 times. ** $p < 0.01$.

circ-LDLRAD3 (Fig. 6A), and the dual-luciferase reporter gene system results validated the above binding sites (Fig. 6B). Specifically, transfection of miR-137 mimic (5 nM, 24 h) significantly decreased the luciferase activity in NSCLC cells co-transfected with wt-LDLRAD3 vectors (5 nM, 24 h), instead of Mut-LDLRAD3 (5 nM, 24 h) (Fig. 6B). Besides, the siRNA for circ-LDLRAD3 (10 nM, 48 h) and OE-circ-LDLRAD3 vectors (10 nM, 48 h) were transfected into the NSCLC cells (Fig. S3A), and the Real-Time qPCR results showed that overexpressed circ-LDLRAD3 inhibited the levels of miR-137 (fold changes: 0.51 and 0.43, vs. Control group), which were increased by downregulating circ-LDLRAD3 (fold changes: 2.31 and 2.19, vs. Control group) in both A549 and H1299 cells (Fig. 6C,D). However, alteration of miR-137 had little effects on circ-LDLRAD3 levels in NSCLC cells (Fig. S3C).

SLC1A5 was identified as the downstream target of miR-137 in the previous study [35]. This study also predicted

the binding sites of miR-137 and 3' UTR regions of SLC1A5 mRNA by using the online StarBase software (<http://starbase.sysu.edu.cn/>) (Fig. 6E). The dual-luciferase reporter gene system results showed that miR-137 mimic (5 nM, 24 h) decreased luciferase activity in NSCLC cells by binding to the predicted sites in Wt-SLC1A5 mRNA (Fig. 6F,G). Further results validated that miR-137 negatively regulated SLC1A5 expressions in NSCLC cells (Fig. 6H-K). Specifically, the results showed that miR-137 over-expression significantly decreased the mRNA (fold changes: 0.53 and 0.61, vs. Control group) and protein (fold changes: 0.48 and 0.34, vs. Control group) levels of SLC1A5 in both A549 and H1299 cells (Fig. 6H-K). Similarly, knock-down of miR-137 promoted SLC1A5 mRNA (fold changes: 1.21 and 1.33, vs. Control group) and protein (fold changes: 1.43 and 1.38, vs. Control group) expressions in NSCLC cells (Fig. 6H-K). Notably, silencing circ-LDLRAD3 inhibited (fold changes: 0.43 and 0.38, vs. Control group), and

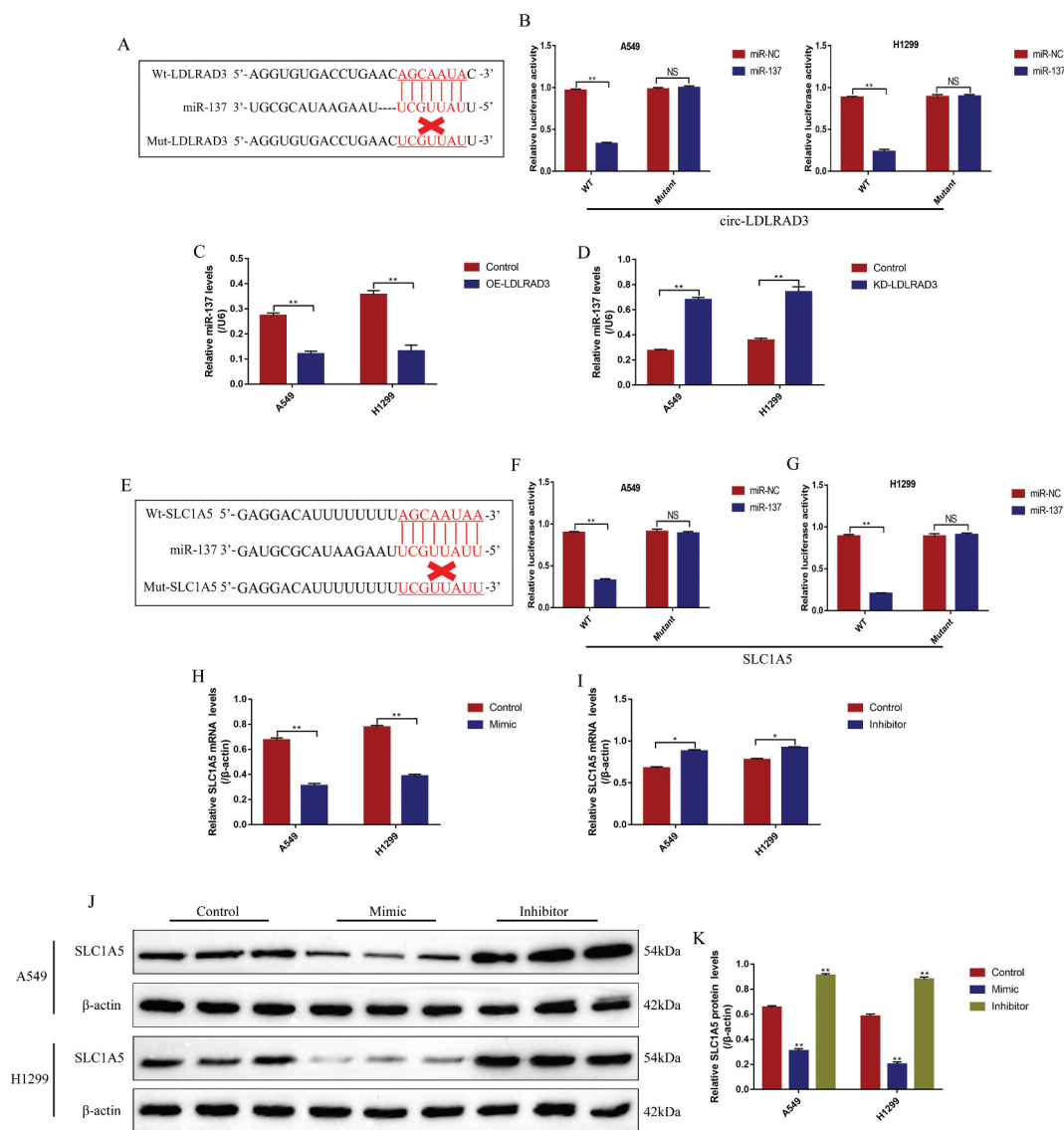


Figure 6. The regulating mechanisms of circ-LDLRAD3, miR-137 and SLC1A5. (A) The online starBase software was used to predict the targeting sites of circ-LDLRAD3 and miR-137. (B) Dual-luciferase reporter gene system was used to verify the binding sites of circ-LDLRAD3 and miR-137. (C, D) Overexpression of circ-LDLRAD3 inhibited miR-137 levels in NSCLC cells, and knock-down of circ-LDLRAD3 had opposite effects. (E) The binding sites of miR-137 and 3' UTR regions of SLC1A5 mRNA were predicted. (F, G) Dual-luciferase reporter gene system was used to verify the binding sites of miR-137 and 3' UTR regions of SLC1A5 mRNA. (H, I) Real-Time qPCR was employed to explore the effects of miR-137 on SLC1A5 mRNA levels in NSCLC cells. (J, K) MiR-137 overexpression inhibited SLC1A5 protein levels in NSCLC cells, while knock-down of miR-137 had the opposite effects. Each experiment repeated at least 3 times. ** $p < 0.01$ and 'NS' represented 'No statistical significance'.

overexpressed circ-LDLRAD3 promoted (fold changes: 1.23 and 1.39, vs. Control group) SLC1A5 expressions in A549 and H1299 cells (Fig. 7A,B). In addition, the promoting effects of circ-LDLRAD3 overexpression on SLC1A5 were abrogated by overexpressing miR-137 in A549 (fold changes: 0.72 and 0.48, vs. OE-LDLRAD3 group) and H1299 (fold changes: 0.81 and 0.65, vs. OE-LDLRAD3 group) cells at both transcriptional (Fig. 7C) and translated levels (Fig. 7E,F). In addition, as shown in Fig. 7D, knock-down of miR-137 restored SLC1A5 mRNA levels in circ-LDLRAD3-deficient NSCLC cells (Fold changes: 1.45 and 2.18, vs. KD-LDLRAD3 group). Interestingly, SLC1A5 mRNA was found to be high-expressed in clinical cancer tissues compared to the paired normal tissues (Fig. 7G). In

addition, high-expressed SLC1A5 mRNA was observed in patients with high-grade TNM stage and lymphatic metastasis (Fig. S4A,B), but the levels of SLC1A5 mRNA were irrelevant to other clinical features, including age, gender, pathological type and smoking status (Fig. S4C-F). Finally, the levels of SLC1A5 mRNA positively correlated with circ-LDLRAD3, but negatively correlated with miR-137 in NSCLC tissues (Fig. 7H,I).

Circ-LDLRAD3 regulated NSCLC cell functions by targeting miR-137 and SLC1A5

We next explored whether circ-LDLRAD3 regulated cell proliferation, apoptosis and invasion by targeting miR-137/SLC1A5

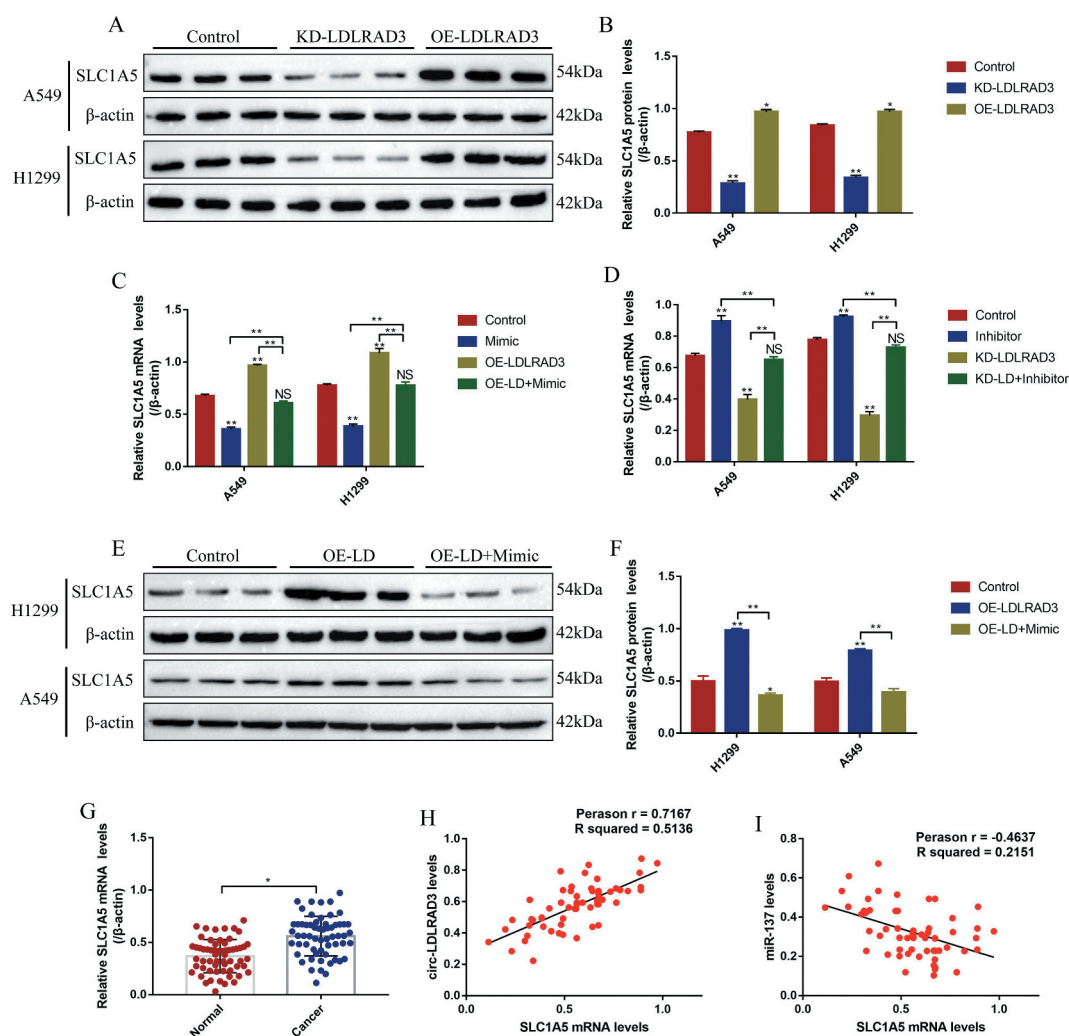


Figure 7. Circ-LDLRAD3 regulated SLC1A5 by sponging miR-137 in NSCLC cells. (A, B) SLC1A5 was positively regulated by circ-LDLRAD3 in NSCLC cells (A549 and H1299). (C, D) The expression levels of SLC1A5 mRNA were regulated by circ-LDLRAD3 through miR-137 in NSCLC cells. (E, F) Western Blot was conducted to determine the expression levels of SLC1A5 protein in NSCLC cells. (G) The expression status of SLC1A5 mRNA in the cancer tissues and adjacent normal tissues collected from NSCLC patients. The Pearson correlation analysis was performed to determine the correlations between (H) SLC1A5 mRNA and circ-LDLRAD3, and (I) SLC1A5 mRNA and miR-137, respectively. Each experiment repeated at least 3 times. * $p < 0.05$, ** $p < 0.01$ and 'NS' represented 'No statistical significance'.

axis. The CCK-8 assay results showed that knock-down of circ-LDLRAD3 inhibited NSCLC cell proliferation in a time dependent manner, which were reversed by both knocking down miR-137 and overexpressing SLC1A5 (Fig. 8A,B). Besides, the colony formation assay results showed that knock-down of circ-LDLRAD3 significantly inhibited colony formation abilities in NSCLC cells, which were also restored by downregulating miR-137 and overexpressing SLC1A5 (Fig. 8C,D). The above results were validated by the Western Blot analysis. Specifically, the inhibiting effects of circ-LDLRAD3 downregulation on Cyclin D1 levels in NSCLC cells were abrogated by knocking down miR-137 (Fold changes: 3.58 and 1.98, vs. KD-LDLRAD3 group) and overexpressing SLC1A5 (Fold changes: 3.64 and 1.73, vs. KD-LDLRAD3 group) in A549 and H1299 cells (Fig. S5A,B). In addition, the TUNEL results showed that deficiency of circ-LDLRAD3 caused significant increase in NSCLC cell apoptosis ratio, which were decreased by downregulating miR-137 and upregulating SLC1A5 (Fig. 8E,F). Also, the promoting effects of circ-LDLRAD3 downregulation on cleaved caspase-3 expressions were abrogated by transfecting cells with miR-137 inhibitor

(Fold changes: 0.84, vs. KD-LDLRAD3 group) and OE-SLC1A5 vectors (Fold changes: 0.82, vs. KD-LDLRAD3 group) in A549 cells (Fig. S5C,D). Furthermore, the inhibiting effects of silencing circ-LDLRAD3 on cell invasion were reversed by both knocking down miR-137 and overexpressing SLC1A5 in A549 and H1299 cells (Fig. 8G,H). Similarly, the inhibiting effects of circ-LDLRAD3 ablation on N-cadherin expressions were reversed by transfecting NSCLC cells with miR-137 inhibitor (Fold changes: 2.85 and 2.31, vs. KD-LDLRAD3 group) and SLC1A5 overexpression vectors (Fold changes: 3.03 and 2.16, vs. KD-LDLRAD3 group) in A549 and H1299 cells (Fig. S5E,F).

Discussion

Circular RNAs (circRNAs) participate in the regulation of cancer progression by acting as post-transcriptional regulators [7–9], and circ-LDLRAD3 has been identified as an oncogene and promoted the development of pancreatic cancer [12,38]. In the present study, we validated that circ-LDLRAD3 also played an oncogenic role to promote non-small cell lung cancer (NSCLC) progression.

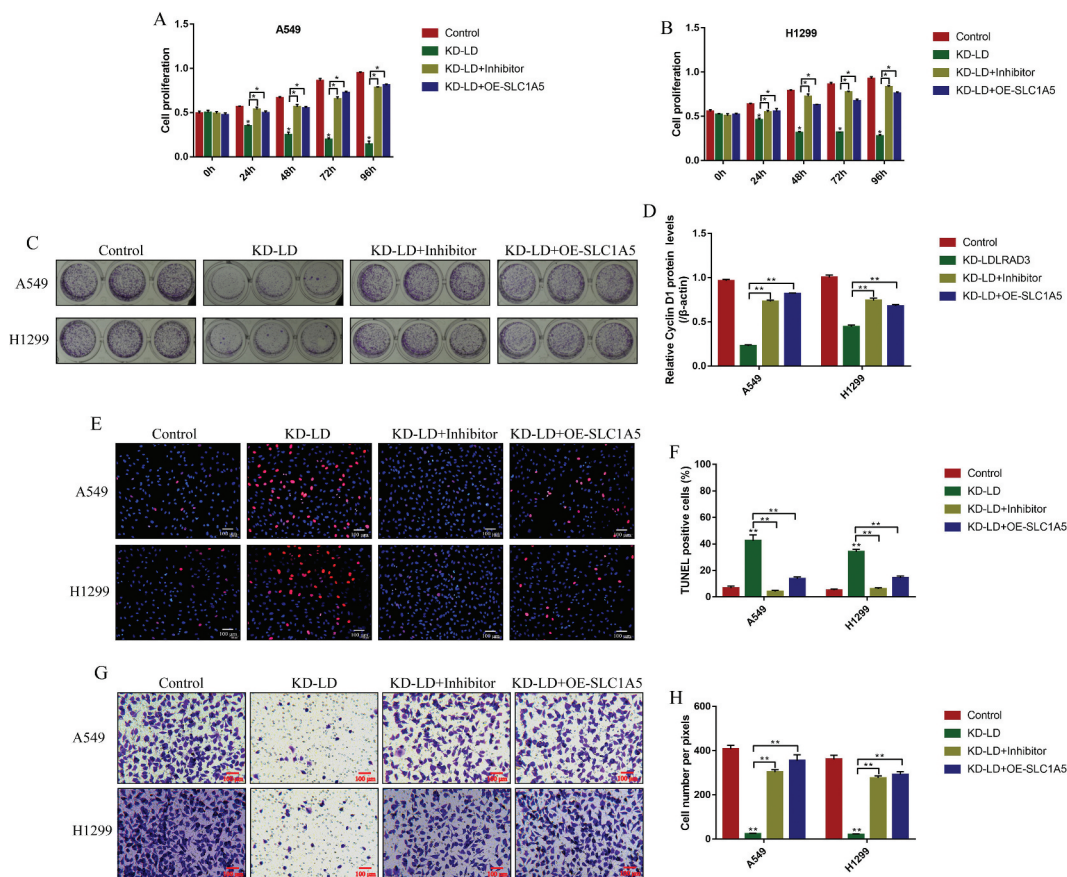


Figure 8. Knock-down of Circ-LDLRAD3 regulated cell functions in NSCLC cells by regulating miR-137/SLC1A5 axis. NSCLC cell proliferation was determined by CCK-8 assay in (A) A549 cells and (B) H1299 cells. (C, D) Colony formation assay was employed to evaluate the colony formation abilities in NSCLC cells. (E, F) TUNEL assay was performed to detect cell apoptosis in NSCLC cells (A549 and H1299). (G, H) The cell invasion abilities for A549 and H1299 cells were determined by Transwell assay. Each experiment repeated at least 3 times. * $p < 0.05$, ** $p < 0.01$.

Mechanistically, by analysing its expression patterns, we found that circ-LDLRAD3 was highly expressed in NSCLC cancer tissues and cell lines compared to their paired normal counterparts. In addition, circ-LDLRAD3 tended to be enriched in patients with high-grade TNM stage and lymphatic metastasis, but was irrelevant to other clinicopathological parameters, including age, gender, pathological type and smoking status, indicating that circ-LDLRAD3 was closely associated with NSCLC pathogenesis. Next, the regulating mechanisms of circ-LDLRAD3 on NSCLC cell functions were investigated by conducting the gain- and loss-function experiments. As expected, we found that knock-down of circ-LDLRAD3 promoted cell apoptosis, inhibited cell proliferation and mobility in NSCLC cells. Consistently, circ-LDLRAD3 overexpression had opposite effects on the above cell functions, indicating that circ-LDLRAD3 slowed down NSCLC progression *in vitro*, which was in consistent with the previous studies in pancreatic cancer [12,38]. Also, the above information enlightened us that circ-LDLRAD3 might be utilized as a potential diagnostic and therapeutic agent for both pancreatic cancer and NSCLC, however, future work is still needed to investigate this issue.

MiR-137 acts as a tumour suppressor to inhibit the development of NSCLC [19,39,40], which was also verified in the present study. Initially, low-expressed miR-137 was observed in NSCLC tissues and cells compared to their normal counterparts, and miR-137 negatively correlated with TNM stage and lymphatic metastasis in clinical specimens, suggesting that miR-137 was a potential

diagnostic biomarker for NSCLC and were in line with the previous work [19,39,40]. In addition, this *in vitro* study also validated that NSCLC cell viability and mobility were inhibited by miR-137 overexpression and promoted by miR-137 downregulation, implying that upregulation of miR-137 hindered NSCLC development *in vitro*. Furthermore, previous studies proved that circ-LDLRAD3 functioned as a competing endogenous RNA to sponge miR-137 [38], and circ-LDLRAD3 promoted pancreatic cancer development through downregulating miR-137 [38]. Consistently, this study validated that circ-LDLRAD3 negatively regulated miR-137, but miR-137 did not affect circ-LDLRAD3 expressions in NSCLC cells. Furthermore, we proved that circ-LDLRAD3 regulated NSCLC cell functions by downregulating miR-137. Mechanistically, the inhibiting effects of downregulated circ-LDLRAD3 on NSCLC cell viability, invasion and epithelial-mesenchymal transition (EMT) were all reversed by knocking down miR-137, indicating that circ-LDLRAD3 silence inhibited malignant phenotypes in NSCLC by upregulating miR-137 and in line with the previous study in pancreatic cancer [38].

Glutamine transporter solute carrier family A1 member 5 (SLC1A5) involves in the regulation of cancer progression [24], which regulates cancer cell growth [25,26] and mobility [29,41,42]. Of note, previous data suggested that SLC1A5 promoted NSCLC cell proliferation [31,32] and metastasis [43], which was validated in this study. Specifically, by analysing the expression patterns of SLC1A5 in the clinical specimens, we found that SLC1A5 was

highly expressed in NSCLC tissues, instead of the normal adjacent tissues, and the expression levels of SLC1A5 were positively correlated with the clinical features, including TNM stage and lymphatic metastasis. Interestingly, SLC1A5 was the downstream target of miR-137 [35,44], and silencing of miR-137 upregulated SLC1A5 to enhance tumour glutamine metabolism [44]. As expected, this study proved that miR-137 functioned as a post-transcriptional regulator to silence SLC1A5 through targeting its 3' untranslated regions (UTR), and circ-LDLRAD3 positively regulated SLC1A5 in NSCLC cells by sponging miR-137. Finally, we proved that knock-down of circ-LDLRAD3 brought detrimental effects to NSCLC cell functions through downregulating SLC1A5. Interestingly, recent data suggested that SLC1A5 contributed to cancer progression by regulating transportation and metabolism of L-glutamine (Gln) [24]. However, more experiments are still needed to investigate whether circ-LDLRAD3/miR-137/SLC1A5 axis regulated NSCLC cell functions by affecting glutamine metabolism in our future work.

To sum up, this *in vitro* study proved that knock-down of circ-LDLRAD3 inhibited cell viability and mobility to slow down NSCLC progression by silencing SLC1A5 through upregulating miR-137, which gave some insights into the underlying mechanisms of NSCLC pathogenesis.

Acknowledgments

This study was financially supported by Scientific Research Projects of Shanghai Municipal Health Committee (No. 201940102).

Disclosure statement

No potential conflict of interest was reported by the authors.

Funding

This work was supported by the Scientific Research Projects of Shanghai Municipal Health Committee [201940102].

ORCID

Xiwen Gao  <http://orcid.org/0000-0002-8377-409X>

References

- Harrison PT, Vyse S, Huang PH. Rare epidermal growth factor receptor (EGFR) mutations in non-small cell lung cancer. *Semin Cancer Biol.* 2019;61:167–179.
- Lou B, Wei D, Zhou X, et al. Long non-coding RNA KDM5B anti-sense RNA 1 enhances tumor progression in non-small cell lung cancer. *J Clin Lab Anal.* 2019;34(1):e22897.
- Wang M, Mao C, Ouyang L, et al. Long noncoding RNA LINC00336 inhibits ferroptosis in lung cancer by functioning as a competing endogenous RNA. *Cell Death Differ.* 2019;26(11):2329–2343.
- Hellmann MD, Paz-Ares L, Bernabe Caro R, et al. Nivolumab plus Ipilimumab in advanced non-small-cell lung cancer. *N Engl J Med.* 2019;381(21):2020–2031. DOI:10.1056/NEJMoa1910231.
- van Timmeren JE, van Elmpt W, de Ruyscher D, et al. Tumor regression during radiotherapy for non-small cell lung cancer patients using cone-beam computed tomography images. *Strahlenther Onkol.* 2019;196(2):159–171.
- Visser S, Koolen SLW, de Bruijn P, et al. Pemetrexed exposure predicts toxicity in advanced non-small-cell lung cancer: A prospective cohort study. *Eur J Cancer.* 2019;121:64–73.
- Jin M, Shi C, Yang C, et al. Upregulated circRNA ARHGAP10 predicts an unfavorable prognosis in NSCLC through regulation of the miR-150-5p/GLUT-1 axis. *Mol Ther Nucleic Acids.* 2019;18:219–231.
- Liu C, Zhang Z, Qi D. Circular RNA hsa_circ_0023404 promotes proliferation, migration and invasion in non-small cell lung cancer by regulating miR-217/ZEB1 axis. *Onco Targets Ther.* 2019;12:6181–6189.
- Liu YT, Han X-H, Xing P-Y, et al. Circular RNA profiling identified as a biomarker for predicting the efficacy of Gefitinib therapy for non-small cell lung cancer. *J Thorac Dis.* 2019;11(5):1779–1787. DOI:10.21037/jtd.2019.05.22.
- Wang Y, Li Y, He H, et al. Circular RNA circ-PRMT5 facilitates non-small cell lung cancer proliferation through upregulating EZH2 via sponging miR-377/382/498. *Gene.* 2019;720:144099.
- Wei S, Zheng Y, Jiang Y, et al. The circRNA circPTPRA suppresses epithelial-mesenchymal transitioning and metastasis of NSCLC cells by sponging miR-96-5p. *EBioMedicine.* 2019;44:182–193.
- Yang F, Liu D-Y, Guo J-T, et al. Circular RNA circ-LDLRAD3 as a biomarker in diagnosis of pancreatic cancer. *World J Gastroenterol.* 2017;23(47):8345–8354. DOI:10.3748/wjg.v23.i47.8345.
- Yao J, Zhang C, Chen Y, et al. Downregulation of circular RNA circ-LDLRAD3 suppresses pancreatic cancer progression through miR-137-3p/PTN axis. *Life Sci.* 2019;239:116871.
- Chen S, Shi F, Zhang W, et al. miR-744-5p inhibits non-small cell lung cancer proliferation and invasion by directly targeting PAX2. *Technol Cancer Res Treat.* 2019;18:1533033819876913.
- Halvorsen AR, Ragle Aure M, Øjlert ÅK, et al. Identification of microRNAs involved in pathways which characterize the expression subtypes of NSCLC. *Mol Oncol.* 2019;13(12):2604–2615. DOI:10.1002/1878-0261.12571.
- Wang YF, Ao X, Liu Y, et al. MicroRNA-608 promotes apoptosis in non-small cell lung cancer cells treated with doxorubicin through the inhibition of TFAP4. *Front Genet.* 2019;10:809.
- Wei C, Zhang R, Cai Q, et al. MicroRNA-330-3p promotes brain metastasis and epithelial-mesenchymal transition via GRIA3 in non-small cell lung cancer. *Aging (Albany NY).* 2019;11(17):6734–6761. DOI:10.18632/aging.102201.
- Fu Y, Yin Y, Peng S, et al. Small nucleolar RNA host gene 1 promotes development and progression of colorectal cancer through negative regulation of miR-137. *Mol Carcinog.* 2019;58(11):2104–2117. DOI:10.1002/mc.23101.
- Chen R, Zhang Y, Zhang C, et al. miR-137 inhibits the proliferation of human non-small cell lung cancer cells by targeting SRC3. *Oncol Lett.* 2017;13(5):3905–3911.
- Yang YR, Li Y-X, Gao X-Y, et al. MicroRNA-137 inhibits cell migration and invasion by targeting bone morphogenetic protein-7 (BMP7) in non-small cell lung cancer cells. *Int J Clin Exp Pathol.* 2015;8(9):10847–10853.
- Li C, Wang Z, Zhang J, et al. Crosstalk of mRNA, miRNA, lncRNA, and circRNA and their regulatory pattern in pulmonary fibrosis. *Mol Ther Nucleic Acids.* 2019;18:204–218.
- Naser Al Deen N, AbouHaidar M, Talhouk R. Connexin43 as a tumor suppressor: proposed connexin43 mRNA-circularRNAs-microRNAs axis towards prevention and early detection in breast cancer. *Front Med (Lausanne).* 2019;6:192.
- Zhang Q, Zhang C, Ma J-X, et al. Circular RNA PIP5K1A promotes colon cancer development through inhibiting miR-1273a. *World J Gastroenterol.* 2019;25(35):5300–5309. DOI:10.3748/wjg.v25.i35.5300.
- Yang Geldermalsen M, Wang Q, Nagarajah R, et al. ASCT2/SLC1A5 controls glutamine uptake and tumour growth in triple-negative basal-like breast cancer. *Oncogene.* 2016;35(24):3201–3208. DOI:10.1038/ncr.2015.381.

- [25] Gkiouli M, Biechl P, Eisenreich W, et al. Diverse roads taken by (13)C-glucose-derived metabolites in breast cancer cells exposed to limiting glucose and glutamine conditions. *Cells*. 2019;8(10):1113.
- [26] Kappler M, Pabst U, Weinholdt C, et al. Causes and consequences of A glutamine induced normoxic HIF1 activity for the tumor metabolism. *Int J Mol Sci*. 2019;20(19):4742. DOI:10.3390/ijms20194742.
- [27] Ding J, Gou Q, Jin J, et al. Metformin inhibits PPARdelta agonist-mediated tumor growth by reducing Glut1 and SLC1A5 expressions of cancer cells. *Eur J Pharmacol*. 2019;857:172425.
- [28] Osman I, He X, Liu J, et al. TEAD1 (TEA domain transcription factor 1) promotes smooth muscle cell proliferation through upregulating SLC1A5 (Solute carrier family 1 member 5)-mediated glutamine uptake. *Circ Res*. 2019;124(9):1309–1322. DOI:10.1161/CIRCRESAHA.118.314187.
- [29] Zhuang X, Tong H, Ding Y, et al. Long noncoding RNA ABHD11-AS1 functions as a competing endogenous RNA to regulate papillary thyroid cancer progression by miR-199a-5p/SLC1A5 axis. *Cell Death Dis*. 2019;10(8):620. DOI:10.1038/s41419-019-1850-4.
- [30] Rajasinghe LD, Hutchings M, Gupta SV. Delta-tocotrienol modulates glutamine dependence by inhibiting ASCT2 and LAT1 Transporters in Non-Small Cell Lung Cancer (NSCLC) cells: a metabolomic approach. *Metabolites*. 2019;9(3):50.
- [31] Hassanein M, Qian J, Hoeksema MD, et al. Targeting SLC1a5-mediated glutamine dependence in non-small cell lung cancer. *Int J Cancer*. 2015;137(7):1587–1597. DOI:10.1002/ijc.29535.
- [32] Hassanein M, Hoeksema MD, Shiota M, et al. SLC1A5 mediates glutamine transport required for lung cancer cell growth and survival. *Clin Cancer Res*. 2013;19(3):560–570. DOI:10.1158/1078-0432.CCR-12-2334.
- [33] Ergun S, Güney S, Temiz E, et al. Significance of miR-15a-5p and CNKSR3 as novel prognostic biomarkers in non-small cell lung cancer. *Anticancer Agents Med Chem*. 2018;18(12):1695–1701.
- [34] Jiang S, Yan W, Wang SE, et al. Let-7 suppresses B cell activation through restricting the availability of necessary nutrients. *Cell Metab*. 2018;27(2):393–403. e4. DOI:10.1016/j.cmet.2017.12.007.
- [35] Luo M, Wu L, Zhang K, et al. miR-137 regulates ferroptosis by targeting glutamine transporter SLC1A5 in melanoma. *Cell Death Differ*. 2018;25(8):1457–1472. DOI:10.1038/s41418-017-0053-8.
- [36] Peng YK, Pu K, Su H-X, et al. Circular RNA hsa_circ_0010882 promotes the progression of gastric cancer via regulation of the PI3K/Akt/mTOR signaling pathway. *Eur Rev Med Pharmacol Sci*. 2020;24(3):1142–1151. DOI:10.26355/eurev_202002_20165.
- [37] Sun X, Luo L, Gao Y. Circular RNA PVT1 enhances cell proliferation but inhibits apoptosis through sponging microRNA-149 in epithelial ovarian cancer. *J Obstet Gynaecol Res*. 2020;46(4):625–635.
- [38] Yao J, Zhang C, Chen Y, et al. Downregulation of circular RNA circ-LDLRAD3 suppresses pancreatic cancer progression through miR-137-3p/PTN axis. *Life Sci*. 2019;239:116871.
- [39] Lu Z, Wang M, Wu S, et al. MicroRNA-137-regulated AKT serine/threonine kinase 2 inhibits tumor growth and sensitizes cisplatin in patients with non-small cell lung cancer. *Oncol Lett*. 2018;16(2):1876–1884. DOI:10.3892/ol.2018.8823.
- [40] Wang X, Zhang G, Cheng Z, et al. Knockdown of LncRNA-XIST suppresses proliferation and TGF-beta1-induced EMT in NSCLC through the Notch-1 pathway by regulation of miR-137. *Genet Test Mol Biomarkers*. 2018;22(6):333–342. DOI:10.1089/gtmb.2018.0026.
- [41] Broer A, Gauthier-Coles G, Rahimi F, et al. Ablation of the ASCT2 (SLC1A5) gene encoding a neutral amino acid transporter reveals transporter plasticity and redundancy in cancer cells. *J Biol Chem*. 2019;294(11):4012–4026. DOI:10.1074/jbc.RA118.006378.
- [42] Lu J, Chen M, Tao Z, et al. Effects of targeting SLC1A5 on inhibiting gastric cancer growth and tumor development in vitro and in vivo. *Oncotarget*. 2017;8(44):76458–76467. DOI:10.18632/oncotarget.19479.
- [43] Csanadi A, Oser A, Aumann K, et al. Overexpression of SLC1a5 in lymph node metastases outperforms assessment in the primary as a negative prognosticator in non-small cell lung cancer. *Pathology*. 2018;50(3):269–275. DOI:10.1016/j.pathol.2017.10.016.
- [44] Dong J, Xiao D, Zhao Z, et al. Epigenetic silencing of microRNA-137 enhances ASCT2 expression and tumor glutamine metabolism. *Oncogenesis*. 2017;6(7):e356. DOI:10.1038/oncsis.2017.59.